

Experimental study of influence of nonlinear effects on phase-sensitive optical time-domain reflectometer operating range

E T Nesterov¹, A A Zhirnov¹, K V Stepanov¹, A B Pnev¹, V E Karasik¹,
Ya A Tezadov², E V Kondrashin² and A B Ushakov²

¹ Bauman Moscow State Technical University, 2-nd Baumanskaya st. 5, 105005
Moscow, Russian Federation

² Scientific and Technological Enterprise IRE-Polyus, pl. Vvedenskogo 1, str. 3,
141190 Fryazino, Moscow region, Russian Federation

E-mail: evgeny.t.nesterov@gmail.com

Abstract. This paper presents experimental results of a study the influence of nonlinear effects on the range of the phase-sensitive optical time-domain reflectometer. Results from measurements of the impact of the effects of stimulated Raman scattering, stimulated Brillouin scattering, self-phase modulation, and modulation instability are presented. It is shown that the power of the probe pulse for 200 ns does not exceed ≈ 300 mW.

1. Introduction

Interest in distributed fiber-optic sensors, including a phase-sensitive reflectometer such as the Rayleigh optical time-domain reflectometer (OTDR), has increased over the past two decades. One of examples of a phase-sensitive OTDR – is a vibration sensor. Distributed optical fiber vibration sensors have advantages such as an extensive operating range, a single-ended fiber connection to the interrogator, and the ability to make additional connections to a pre-existing fiber-optic cable. In some cases, the last advantage listed makes a solution cost-effective. Digital electronics development in recent years has enabled practical realization of fiber-optic distributed sensors based on scattering effects [1–12].

The main advantage of distributed fiber-optic sensors is a large operating range. One of the factors limiting the range of the phase-sensitive OTDR is related to the power pulses input into the fiber that are due to the influence of nonlinear effects in the fiber [9, 11, 15–22].

The range of the distributed vibration sensor based on the phase-sensitive Rayleigh OTDR is determined by providing the desired signal-to-noise ratio (SNR) of the system in a given area of the optical fiber. An increase in the SNR can be obtained by decreasing the system's noise power or by increasing the supplied optical probe pulse energy to the fiber. In practice, increasing the probe pulse energy supplied to the optical fiber impulse power (at a fixed duration) leads to a decrease in the power of the backscattered signal. This phenomenon can be explained by appearance of nonlinear effects in optical fiber [14].

In this paper, we present experimental results of a study on the influence of nonlinear effects on the range of a phase-sensitive OTDR. We also present the results of measuring the impact of the effects of stimulated Raman scattering (SRS), stimulated Brillouin scattering (SBS), self-phase modulation (SPM), and modulation instability (MI). The results also show (Figure 2) that the power of the probe pulse duration of 200 ns does not exceed 300 mW.



2. Experiments

To determine the dependence of reflectogram quality on probe pulse power, we built the experimental setup shown in Figure 1.

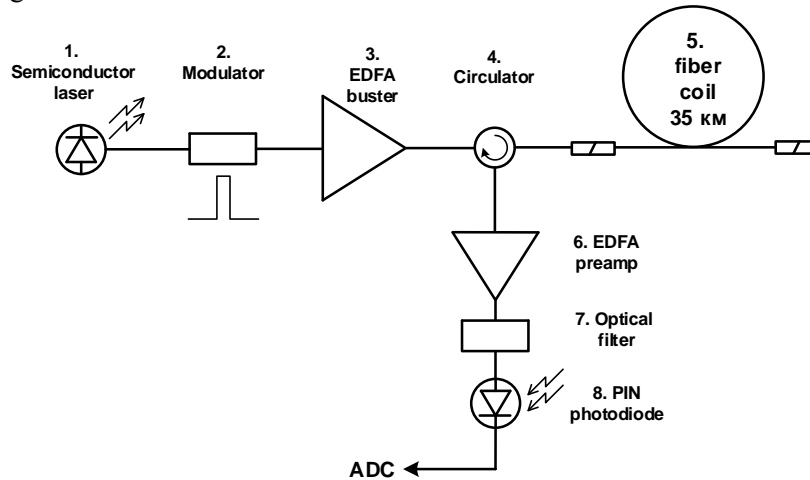


Figure 1. Experimental setup of COTDR: 1 is a light source, 2 is a modulator, 3 is an erbium-doped fiber amplifier (EDFA)-buster, 4 is an optical circulator, 5 is a fiber coil, 6 is an EDFA-preamplifier, 7 is an optical filter, 8 is a PIN photodiode.

Increasing the probe pulse power up to 250 mW (Figure 2 a, b) resulted in an increase of the reflectogram amplitude. Further increasing the power leads to a decrease in reflectogram amplitude, which starts from the end of the connected optical fiber sensor (Figure 2 c, d).

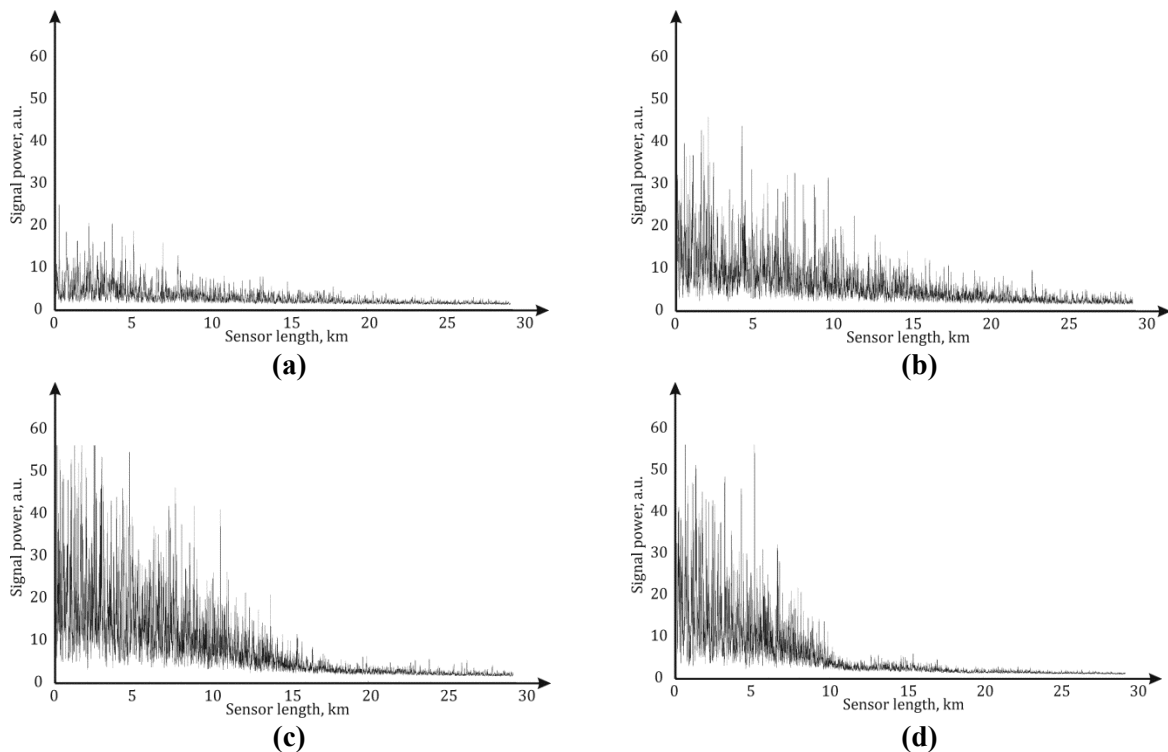


Figure 2. Reflectogram of probe pulse corresponds to: a) $P = 80$ mW, $\tau = 200$ ns, b) $P = 210$ mW, $\tau = 200$ ns, c) $P = 280$ mW, $\tau = 200$ ns, d) $P = 320$ mW, $\tau = 200$ ns.

The decreasing amplitude can be explained by the appearance of nonlinear effects in the silica fiber. The following nonlinear effects are known to be present in the fiber [14]: SRS, SBS, SPM, and four-wave mixing (FWM), which in the case of the signal and the spontaneous emission radiation interaction is called MI. In the next sections, we assess the impact of non-linear effects in the Rayleigh COTDR.

3. Stimulated Raman scattering

SRS is manifested when incident radiation causes radiation generation with a shifted frequency, called Stokes radiation. The magnitude of the frequency shift is determined by the vibrational modes of the medium [14-16].

The probe optical pulse serves as a pump for generating radiation with a shifted frequency in the case of the pulse reflectometer. The weighted average maximum frequency shift is 13.2 THz with respect to the pump radiation frequency. The SRS threshold is defined as the input pump power that generates a Stokes radiation power equal to the output pump power.

Under the assumption of a Lorentzian shape of the gain spectrum, the critical pumping power can be estimated approximately by the formula [15]:

$$P_{SRS} \approx \frac{16A_{eff}}{g_{SRS}L_{eff}} \tag{1}$$

where P_{SRS} is the threshold power, $A_{eff} = 75\mu m^2$ is the effective mode area, $g_{SRS} = 6,5 \times 10^{-14} m/W$ is the gain factor [5], and $L_{eff} = (1 - e^{-\alpha L})/\alpha$ is the effective fiber length; for typical losses in fiber of 0.2 dB/km, $\alpha \approx 4.8 \times 10^{-5} m^{-1}$ and $L_{eff} = 18 km$. Calculation according to Formula 1 gives the result:

$$P_{SRS} \approx 700 mW \tag{2}$$

Our experimental setup for the SRS measurement is shown in Figure 3.

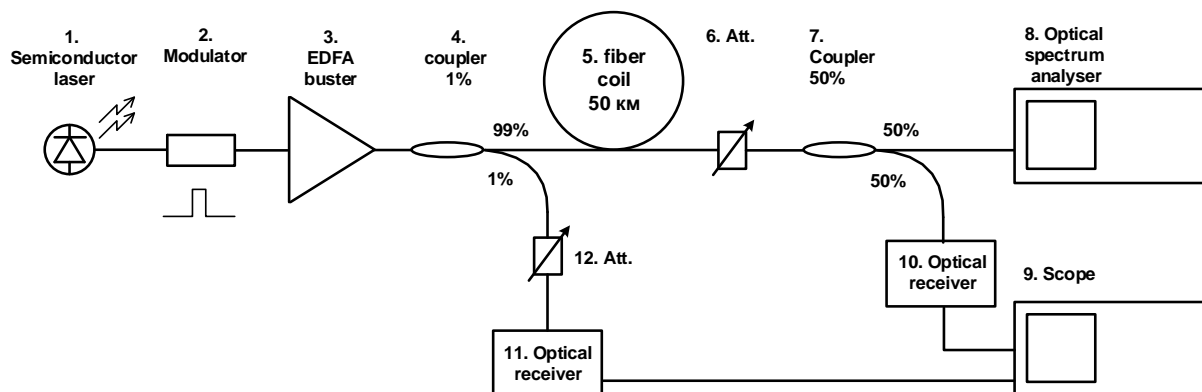


Figure 3. Experimental setup for SRS measurement.

Some of the obtained results of the measurements are shown below in Figures 4(a-d).

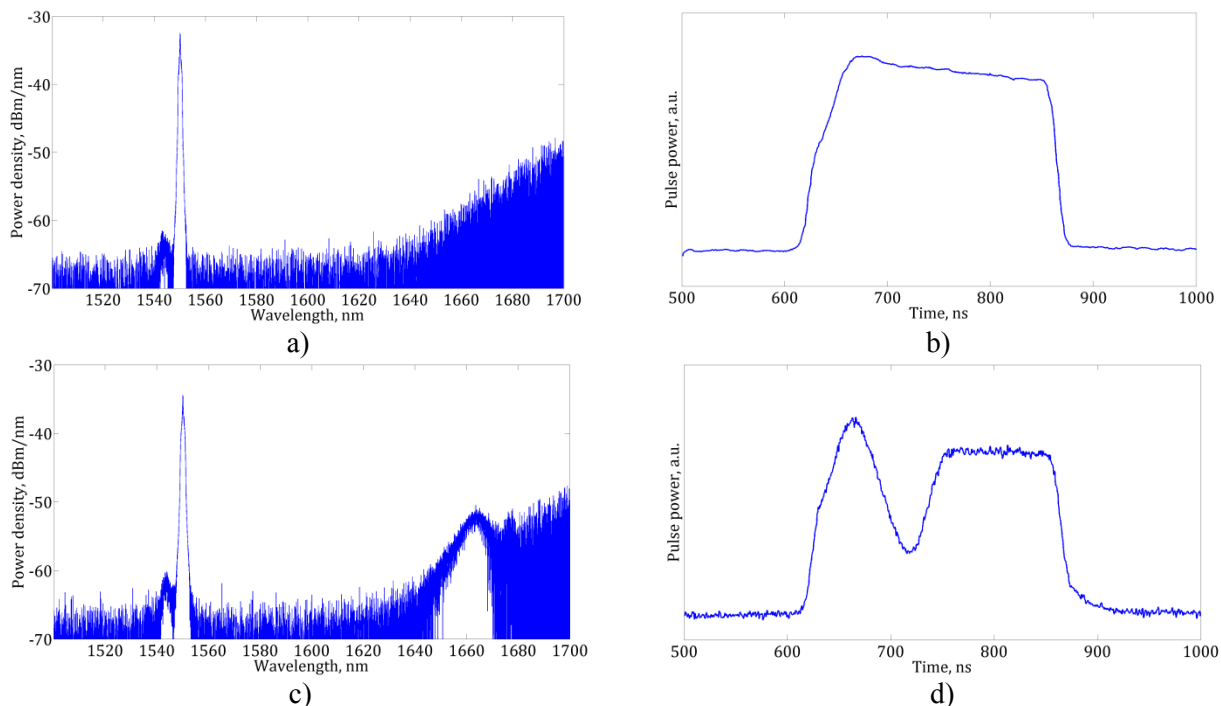


Figure 4. Spectrum (a) and oscillogram (b) of the output pulses corresponds to input power 1.5 W, pulse duration 200 ns. Spectrum (c) and oscillogram (d) of the output pulses corresponds to input power 2 W, pulse duration 200 ns.

As can be seen from Figures 4a-4d SRS begins to develop when the probe pulse power exceeds 1500 mW. That value is two times larger than the theoretical threshold previously calculated (2). The discrepancy between the theoretical calculation and experimental data can be explained by the fact that expression (1) is obtained for the case of continuous pumping. In the case of pulse pumping, the Stokes component is caused by the finite duration pulse. The difference between the Stokes emission wavelength and pump wavelength is about 100 nm (figure 4c). Due to the dispersion component in the fiber $D = 17\text{ps} \times \text{nm}^{-1} \times \text{km}^{-1}$, after passing 50 km of fiber the Stokes wave and the probe pulse after passing undergo an 85-ns time delay (figure 4d).

The increasing of the SRS threshold to a value greater than 1.5 W is explained by finite pulse duration and time delay between probe pulse and generated Stokes wave. The obtained results indicate that SRS is not the main factor of the decrease in the reflectogram amplitude.

4. Stimulated Brillouin scattering

SBS is manifested in the form of Stokes wave propagation in the opposite direction with respect to the pump wave and containing a significant portion of the initial energy. The SBS process can be described classically as a parametric interaction between the pump, Stokes waves, and acoustic waves. Due to electrostriction, a pump wave generates an acoustic wave resulting in a periodic modulation of the refractive index. Induced refractive-index grating reflects the pump radiation [14-16].

The width of the SBS gain spectrum is about 10 MHz. The frequency shift of the reflected wave caused by the Doppler effect is 10 GHz. Only backscatter propagation of SBS is possible in a single-mode fiber. The SBS threshold is determined by the formula [17]:

$$P_{SBS} \approx \frac{21A_{eff}}{g_{SBS}} \frac{n}{Tc'} \quad (3)$$

where P_{SBS} is the threshold power, $A_{eff} = 75\mu m^2$ is the effective mode area, $g_{SBS} = 4,5 \times 10^{-11} m/W$ is the gain [18], $T = 200 ns$ is the pulse duration, $c = 3 \times 10^8 m/s$ is the speed of light in vacuum, $n = 1.5$ is the refractive index of quartz. Using the expression given in (3), we find $P_{SBS} \approx 850 mW$.

The experimental setup for a study of the SBS influence is shown in figure 5.

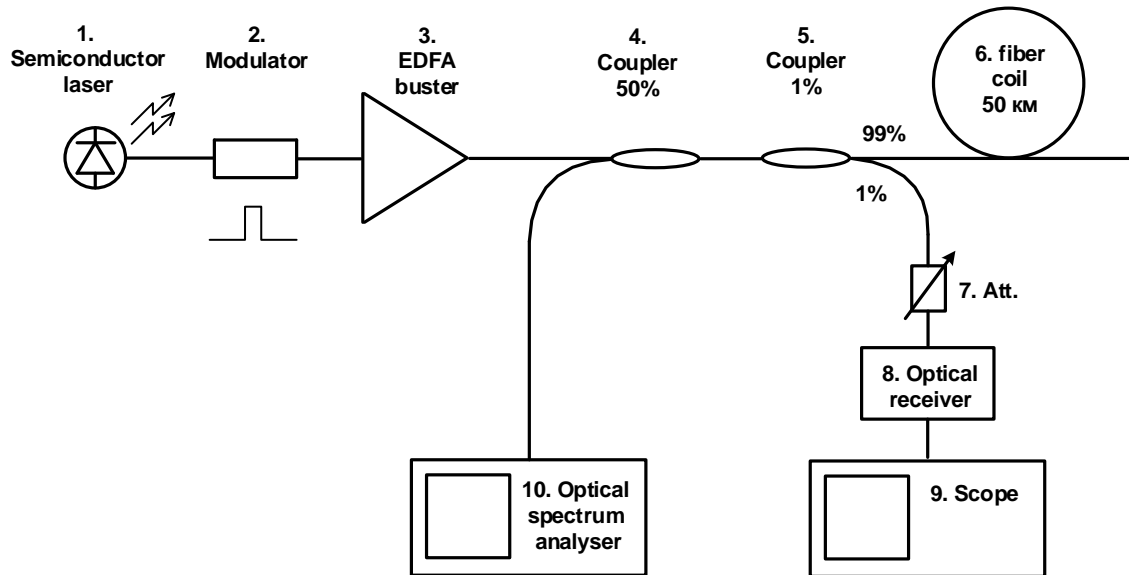


Figure 5. Experimental setup for SBS measurement.

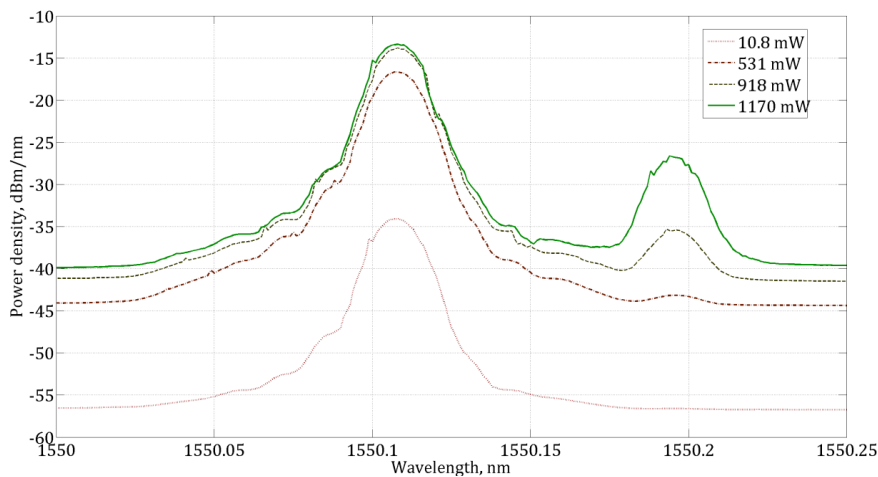


Figure 6. Backscattered spectrum of different input pulse powers.

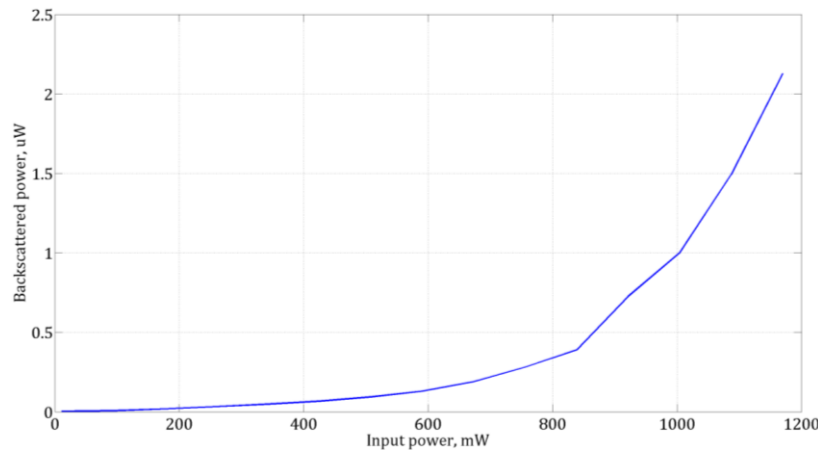


Figure 7. Backscattered power.

On Figure 6 and Figure 7, we can see that SBS begins to develop after the probe pulse power reaches a value of about 850 mW. Hence, SBS is not a main effect leading to a decrease in the reflectogram amplitude as the power of the probe pulse increases.

5. Self-phase modulation

SPM appears to be due to the dependence of the refractive index of quartz from the radiation energy injected into the fiber [14]. SPM causes a frequency shift in the scanning pulse passed through the fiber and can be calculated by equation (4) [19]:

$$\delta\nu = \frac{n_2 L_{\text{eff}} \delta P}{A_{\text{eff}} \lambda \delta t'} \quad (4)$$

where n_2 is the nonlinear refractive index, L_{eff} is the effective fiber length, $A_{\text{eff}} = \pi a_m^2$ is the effective area of the fiber, a_m is the mode radius, λ is the emission wavelength, and P is the power of the optical pulse.

Backscattered Rayleigh radiation contains a frequency shift, which develops in a pulse as it passes through the optical fiber. Backscattered Rayleigh radiation (given to the band receiver) is proportional to the integral of the instantaneous power spectrum over the frequency [20], given by equation (5):

$$F(\delta\nu) = \int_{-1/T}^{1/T} \left[\frac{\sin(\pi(\nu - \delta\nu)T)}{\pi(\nu - \delta\nu)T} \right]^2 d\nu, \quad (5)$$

where ν is the frequency, T is the pulse duration, $\Delta F = 1/T$ is the receiver bandwidth, and $\delta\nu$ is the frequency shift caused by SPM. The decrease in sensitivity due to the frequency shift is proportional to:

$$d(\delta\nu) = F(\delta\nu)/F(0) \quad (6)$$

Figure 8 presents sensitivity reduction as a function of the ratio of the frequency shift to the electric band receiver tract. The electric band of the receiver tract is determined on the basis of the pulse duration. Therefore, for a pulse duration of $T = 200$ ns, the receiver bandwidth is $\Delta F = 5$ MHz

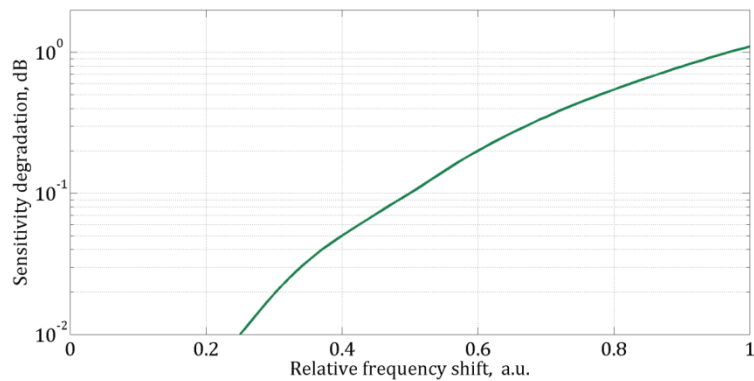


Figure 8. Sensitivity degradation

Our experimental setup was made for the quantitative measurement of the frequency shift $\Delta\nu$. The scheme of the setup is shown in Figure 9.

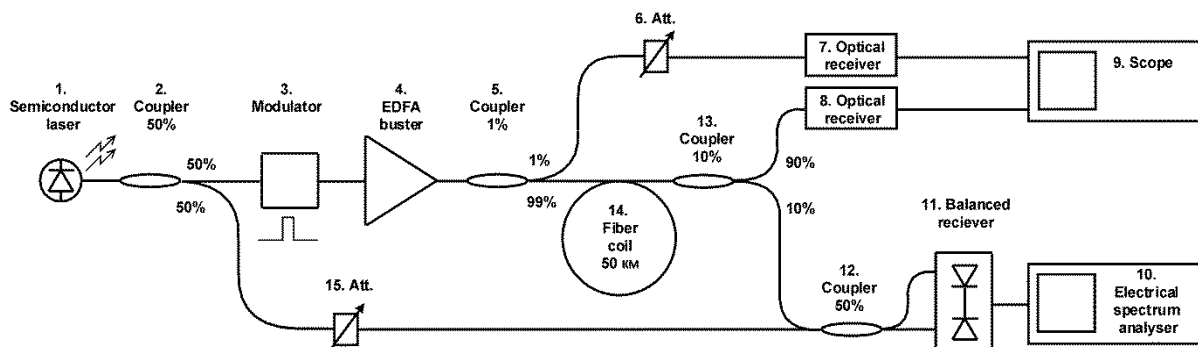


Figure 9. Experimental setup for study of the SPM influence.

The measurement results are shown in figures 10a and 10b below.

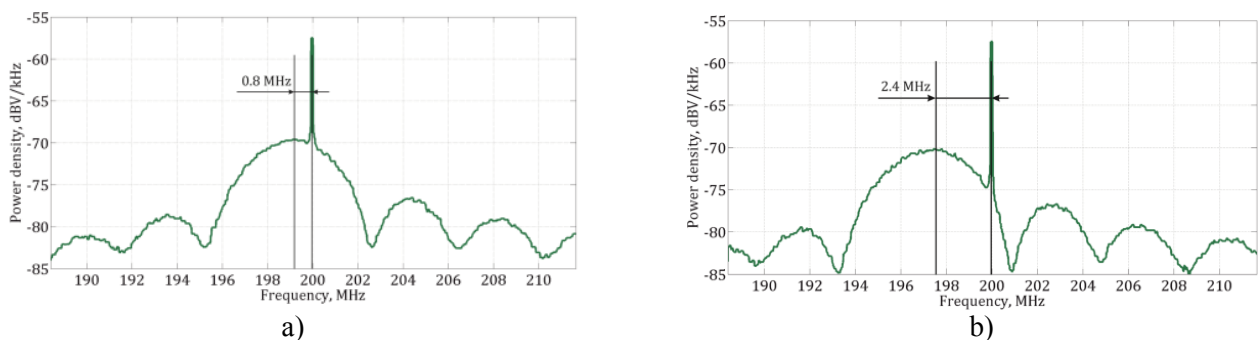


Figure 10. Signal spectrum corresponds to input pulse power: a) 300 mW and b) 500 mW.

As it shown in these figures, if the probe pulse power is 500 mW, then the frequency shift is 2.4 MHz. The sensitivity degradation is 0.1 dB, with $\partial\nu/\Delta F \cong 0.5$. Thus, SPM is not the main nonlinear effect limiting the power of the probe pulse injected into the fiber.

6. Modulation instability

MI is a degenerate case of FWM, representing a parametric amplification of noise [14, 15, 21, 22]. Pulses with power levels of several hundred milliwatts must be input into the optical fiber to ensure a sufficient SNR for backscatter signal processing. Such power levels can be achieved by using an EDFA. Optical amplifiers generate their own spontaneous emission noise. The interaction between signal and spontaneous radiation in the same frequency band, accompanied by the generation of new spectral components, is a degenerate case of FWM [14, 15].

Generation of new spectral components occurs at frequencies symmetrically shifted towards lower and higher frequencies. If the radiation frequency is indicated as ν_0 , the new spectral components are generated at frequencies $\nu_0 + \nu_S$ and $\nu_0 - \nu_S$. The spectral component of the $\nu_0 + \nu_S$ and $\nu_0 - \nu_S$ frequency is called the anti-Stokes and Stokes component, respectively. The value of ν_S is determined by equation (7) [14, 21]:

$$\nu_S = \frac{1}{2\pi} \sqrt{\frac{2\gamma P_i}{|\beta_2|}}, \quad (7)$$

where P_i is the optical power, $\gamma = 2\pi n_2/(\lambda A_{\text{eff}})$ is the nonlinearity parameter, $n_2 = 3.2 \times 10^{-20} \text{m}^2/\text{W}$ is the nonlinear refractive index, $\lambda = 1.5 \mu\text{m}$ is the wavelength, $A_{\text{eff}} = 75 \mu\text{m}^2$ is the effective mode area, and β_2 is the coefficient of the group velocity dispersion calculated using Equation (8).

$$\beta_2 = -\frac{\lambda^2}{2\pi c} D, \quad (8)$$

Also, $D = 17 \text{ps} \times \text{nm}^{-1} \times \text{km}^{-1}$ is the dispersion coefficient and c is the speed of light, as before. Taking into account the above values, we can get

$$\nu_S = 0.12 \text{nm}. \quad (9)$$

The experimental setup for modulation instability study is shown in Figure 11.

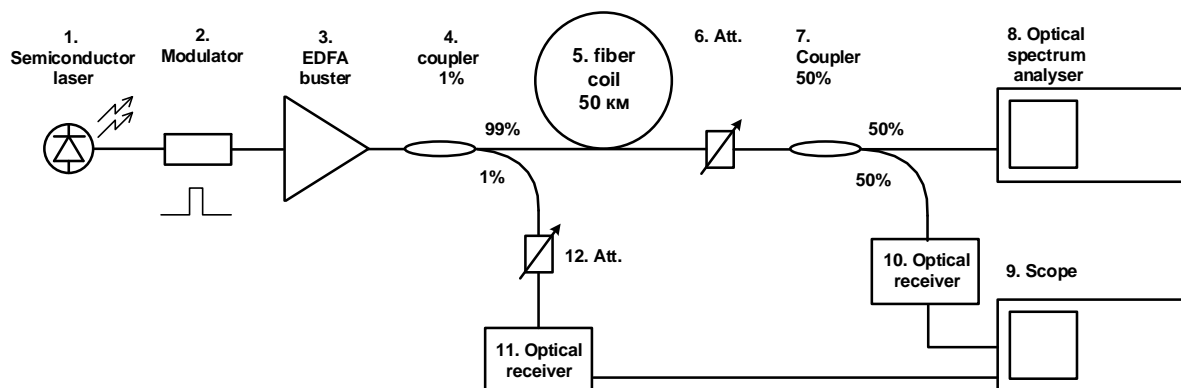


Figure 11. Experimental setup for calculation of backscattered power.

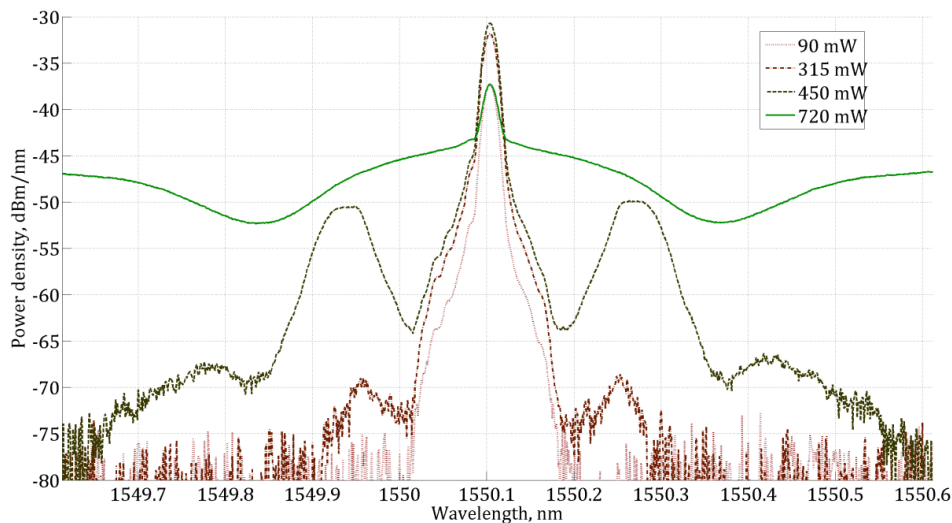


Figure 12. Output spectrum of different input pulse power.

The spectrum of a pulse passed through the 50 km fiber coil is shown in Figure 12. Results obtained from this data lead to the conclusion that Stokes lines appear when pulse power reaches the value of 315 mW. When pulse power reaches 450 mW, the power of the Stokes lines becomes commensurate with the power of radiation with the original input wavelength.

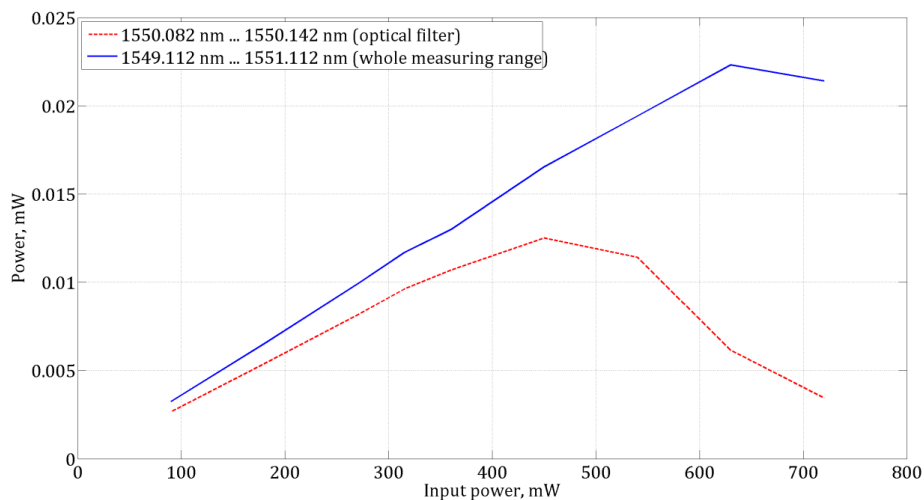


Figure 13. Output power in various ranges.

7. Discussion

An important feature of COTDR is the optical filter installed after pre-EDFA (see Figure 1). It has a bandwidth $\Delta\nu_F \approx 0.07$ nm and reduces the spontaneous emission noise of the fiber amplifier. Stokes lines wavelengths lay outside the range of this optical filter. That is the reason for the decrease in the optical power (Figure 13). As a result, the reflectogram amplitude decreases in the far fiber section (> 10 km) when the probe pulse power exceeds 300 mW.

8. Conclusions

Experimental results of the influence of four non-linear effects – stimulated Raman scattering (SRS), stimulated Brillouin scattering (SBS), self-phase modulation (SPM), and four-wave mixing (FWM)/modulation instability (MI) – on device operation with a scanning pulse duration of 200 ns are

shown. We found that the main nonlinear effect is the MI, whose development is observed when the pulse power reaches 300 mW.

Acknowledgments

This work is supported by the Russian Ministry of Industry and Trade, State Contract № 13411.1007499.09.033. The authors are thankful to Treschikov V. N., Director of the ‘T8’-company, Prof. Listvin V. N., and Prof. Naniy O. E. for useful discussions.

References

- [1] Taylor H F and Lee C E 1993 *US 5194847 A*
- [2] Choi K N, Juarez J C and Taylor H F 2003 *Proc. SPIE* **5090** 134-41
- [3] Juarez J C et al. 2005 *J. Lightwave Technol.* **23** 2081-87
- [4] Juarez J C and Taylor H F 2007 *Appl. Opt.* **46** 1968-70
- [5] Juskaitis R, Mamedov A M, Potapov V T and Shatalin S V 1992 *Opt. Lett.* **17**, 1623
- [6] Healey P and Malyon D J 1982 *Electron. Lett.* **18** 862-63
- [7] Tai K, Hasegawa A and Tomita A 1986 *Phys. Rev. Lett.* **56** 135-38
- [8] Martins H F, Martin-Lopez S and Corredera P 2013 *Opt. Lett.* **38** 872-74
- [9] Lu Y L, Zhu T, Chen L A and Bao X Y 2010 *J. Lightwave Technol.* **28** 3243
- [10] Izumita H, Koyamada Y, Furukawa S and Sankawa I, 1994 *J. Lightwave Technol.* **12** 1230
- [11] Simaeyts G V, Emplit P and Haelterman M 2001 *Phys. Rev. Lett.* **87** 033902
- [12] Simaeyts G V, Emplit P and Haelterman M 2002 *J. Opt. Soc. Am. B* **19** 477
- [13] Alasia D, Herraiez M G, Abrardi L, Lopez S M and Thevenaz L 2005 *Proc. Soc. Photo-Opt. Instrum. Eng.* **5855** 587
- [14] Agrawal G P 2013 *Nonlinear fiber optics* (New York: Academic Press)
- [15] Izumita H, Koyamada Y, Furukawa S I and Sankawa I 1994 *J. Lightwave Technol.* **12** 1230-38
- [16] Smith R G 1972 *Appl. Opt.* **11** 2489-94
- [17] Koyamada Y, Nakamoto H and Ohta N 1992 *J. Opt. Commun.* **13** 127-33
- [18] Stolen R and Rogers H 1980 *Proc. IEEE* **68** 1232-36
- [19] Stolen R and Lin C 1978 *Phys. Rev.* **17** 1448
- [20] Healey P 1984 *Electronics letters – IET* **20** 30-32
- [21] Stolen R and Bjorkholm J 1982 *Quantum Electronics IEEE J.* **18** 1062-72
- [22] Babin S A et al. 2010 *Laser Phys.* **20** 334-40